Article

Amphiphile-Mediated Ultrasmall Aggregation Induced Emission Dots for Ultrasensitive Fluorescence Biosensing

Haiyin Li, Chuanfeng Wang, Ting Hou, and Feng Li

Anal. Chem., **Just Accepted Manuscript** • DOI: 10.1021/acs.analchem.7b01797 • Publication Date (Web): 04 Aug 2017

Amphiphile-Mediated Ultrasmall Aggregation Induced Emission Dots for Ultrasensitive Fluorescence Biosensing

Haiyin Li, Chuanfeng Wang, Ting Hou, and Feng Li*

College of Chemistry and Pharmaceutical Sciences, Qingdao Agricultural University,

Qingdao 266109, People's Republic of China

* Corresponding author. Tel/Fax: 86-532-86080855; E-mail: lifeng@qust.edu.cn

ABSTRACT

The development of ultrasensitive and highly selective fluorescence biosensors for diverse analytes is highly desirable but remains a challenge. It is attributable to the scarcity of fluorogens with promising brightness, stability and nontoxicity, which primarily determine the performance of fluorescence biosensors. Herein, we report the design and preparation of aggregation induced emission (AIE) dots with high brightness, exceptional colloidal stability, ultrasmall size, and functional groups for developing ultrasensitive biosensor through the electrostatic conjugation to biological molecules, and use blemycin (BLM) as the proof-of-concept analyte. The recognition and the subsequent cleavage of the quencher-labelled DNA (Q-DNA) by BLM result in the formation of three-mer quencher-linked oligonucleotide fragments (Q-DNA-1), which significantly decreases the amount of quenchers anchored on AIE dots surface and subsequently reduces the fluorescence resonance energy transfer (FRET) effect. As compared to the case that BLM is absent, remarkable fluorescence enhancement is observed, and is dependent on BLM concentration. Thus, ultrasensitive fluorescence detection of target BLM is realized, with a detection limit down to 3.4 fM, the lowest value reported so far. Moreover, the proposed fluorescence biosensor has also been successfully utilized for detection of BLM spiked in human serum samples. The as-proposed strategy not only significantly improves the selectivity and sensitivity of BLM assay, but also allows the ultrasensitive detection of a variety of bioactive molecules by simply changing the specific target recognition substances, thus providing a versatile fluorescence platform, and showing great potential to be applied in chemo-/bioanalysis and clinical biomedicine.

INTRODUCTION

There is great demand on the design and development of highly sensitive and specific chemo-/biosensors for diverse analytes ranging from small molecules/heavy metal ions to tumor biomarkers.[1] Over the past decade, various biosensing strategies, such as electrochemistry,[2,3] chemiluminescence,[4,5] electro-chemiluminescence,[6,7] and surface plasmon resonance (SPR)[8] have been developed as alternative strategies to conventional assays for analyte detection. In comparison, fluorescence biosensing offers distinct and intrinsic merits in terms of convenience, rapidity, and high sensitivity, which make it a powerful analytical tool in disease diagnosis and fundamental biological studies.[9,10] A variety of fluorescence biosensors, including organic molecule probes,[11-13] metal nanocluster probes,[14] and dye-labelled DNA probes,[15] have been widely developed. Nevertheless, most fluorescence assays are subject to limitations such as weak luminescence, insufficient water solubility/dispersibility, and photobleaching.[16,17] On the other hand, owing to their advantages of excellent photostability, tunable photoluminescence, and ease of preparation, fluorescence nanoaggregates have been regarded as promising fluorogens to construct biosensing platforms.[18,19] Meanwhile, fluorescence nanoaggregates can be modified by changing their structures, sizes and surface functional groups. In this context, recently fluorescence nanoaggregates have drawn much attention for their advanced utilization in cell imaging and bioanalysis.[20,21] However, most fluorescence nanoaggregates previously reported were comprised of inorganic species, even some toxic heavy metal ions (e.g. Cd^{2+}, Pb^{2+}), of which the potential cytotoxicity effects greatly hindered their practical applications. Therefore, it is highly desirable and of great research interest to design and prepare fluorescence nanoaggregates with low toxicity, outstanding biocompatibility and high brightness for practical biomedical applications.

Fluorescence organic nanoaggregates, more interestingly show advantages of low toxicity and good

biocompatibility, making them attractive alternatives for advanced applications in chemo-/bioanalysis.[22,23] Recent efforts have been made to develop fluorescence organic nanoaggregates as fluorescent probes. The commonly used strategies to generate such nanoaggregates included the reprecipitation method and the radical polymerization approach.[24,25] However, poisonous solvent/surfactant was usually used, resulting in serious damage to cells, tissues and organs in biological applications. In addition, they were quite unstable in mixed solution or clinical samples, and prone to aggregate spontaneously into irregular and bulky particles after a certain period of time. Meanwhile, their surface lacked functional groups, and thus it was difficult to modify these nanoaggregates by chemical techniques.

Regarding the fluorescence organic nanoaggregates improvements, fluorescent amphiphiles have been proven to be ideal candidates because they were beneficial for nanoaggregate preparation, improving the stability, increasing biocompatibility and enriching the surface functionality.[26,27] In this context, fluorescent amphiphiles, with well-designed structures and self-assembling behaviour, have attracted great interest among chemists and material scientists in recent years due to their applications in numerous fields including molecule diagnosis and cell imaging.[27] However, low fluorescence quantum yield of the present organic nanoaggregates remains one key drawback, mainly owing to the inherent fluorescence quenching effect of conventional organic dyes. Aggregation induced emission (AIE) fluorogens, first reported by Tang,[28] enjoy prominent fluorescence in aggregate state, which can readily solve the above dilemma, and have been widely applied in numerous fields.[29-32] From this point of view, AIE amphiphiles are extremely promising in preparation of nanoaggregates for advanced application in chemo-/biosensors. However, to the best of our knowledge, there are still many difficulties in preparing nanoaggregates for advanced utilization in detection of diverse analytes. First, very few nanoaggregates meet the safety requirement that requires the fluorogens to be smaller than 10 nm for efficient renal and liver clearance.[33,34] Second, in

addition to fluorescence moieties, such nanoaggregates are also composed of a significant fraction of non-fluorescence moieties, which will obviously decrease the fluorescence brightness of a particle with a given size.[22,23] Third, versatile surface modification and conjugation to bioactive molecules has yet to be further developed.[35,36] In this regards, it remains a great challenge and opportunity to develop AIE nanoaggregates with improved properties and apply them in ultrasensitive fluorescence biosensors.

Herein, a novel class of AIE nanoaggregates with the diameter of about 5 nm, denoted as AIE dots, was successfully prepared through the amphiphile self-assembly, with extraordinary brightness, excellent colloidal stability and nontoxic features. Based on the as-prepared AIE dots, a facile bioconjugation strategy for designing fluorescence bioassay was ingeniously developed through the electrostatic interaction between AIE dots and biological molecules. This strategy can be easily and universally applied to any fluorescence materials with positive charges on the surface. We applied the bioconjugates to ultrasensitive fluorescence biosensing, with bleomycin (BLM) as the proof-of-concept analyte. In the present study, a quencher labeled single-stranded deoxyribonucleic acid (denoted as Q-DNA, containing the target recognition sequence) was ingeniously designed. The proposed biosensor was successfully prepared through the electrostatic adsorption of Q-DNA on AIE dots and exhibited weak fluorescence due to the FRET effect. However, in the presence of BLM, the sequences in Q-DNA can be recognized and cleaved by BLM, thus releasing three-mer quencher-linked oligonucleotide fragments (Q-DNA-1) and subsequently resulting in the separation of AIE dots and quenchers. As a result, the fluorescence intensity increases and is dependent on the BLM concentration. Therefore, by taking advantage of the AIE dots-assisted fluorescence enhancement, ultrasensitive detection of BLM is readily realized using this fluorescence assay.

EXPERIMENTAL SECTION

Preparation of TPEP-2CHO. TPE-2Br (2.45 g) and 4-formylbenzeneboronic acid (1.65 g) were dissolved in toluene (60 mL), followed by addition of 2 M aqueous K_2CO_3 solution (11 mL) and TBAB (0.1 g). After stirred for 30 min under Ar atmosphere, $Pd(PPh_3)_4$ catalyst (catalytic amount) was added and the mixture was allowed to react at 85 °C for 24 h. The product was concentrated and purified by silica gel column chromatography with CH_2Cl_2:n-hexane (v:v, 2:1) as the eluent, and then yellow power was obtained with a yield of 78%. ^{1}H NMR (500 MHz, $CDCl_3$) δ (ppm): 7.08 (dd, 5H), 7.13~7.17 (m, 10H), 7.42 (d, 4H), 7.71 (d, 4H), 7.90 (d, 4H), 10.03 (s, 2H); FT-IR (KBr) ν (cm^{-1}): 2830, 1700, 1600, 1410, 1210, 1110, 835, 696.

Preparation of TPEP-2OH. TPEP-2CHO (1.08 g) was dissolved in methanol (40 mL), followed by addition of $NaBH_4$ (0.30 g). The reaction mixture was slowly warmed up to 65 °C and stirred under Ar atmosphere for 6.0 h. The crude product obtained was purified through recrystallization in methanol, and white power was obtained with a yield of 95%. ^{1}H NMR (500 MHz, $CDCl_3$) δ (ppm): 2.04 (dd, 8H), 4.71 (s, 4H), 7.11 (m, 10H), 7.25 (s, 1H), 7.25 (dd, 6H), 7.55 (d, 3H); FT-IR (KBr) ν (cm^{-1}): 3410, 2960, 1550, 1410, 1040, 1020, 808, 704.

Preparation of TPEP-2CBr. TPEP-2OH (0.82 g) was dissolved in CH_2Cl_2 (30 mL), followed by addition of PBr_3 (1.62 g). The reaction mixture was stirred under Ar atmosphere overnight. Subsequently, the mixture was quenched with water (30 mL). The organic substances were extracted three times with CH_2Cl_2. The product was concentrated and purified by silica gel column chromatography with n-hexane as the eluent to afford TPEP-2CBr as a white power (yield, 93%). ^{1}H NMR (500 MHz, $CDCl_3$) δ (ppm): 4.52 (s, 4H), 7.06~7.13 (m, 13H), 7.25 (s, 1H), 7.35 (d, 4H), 7.41 (d, 4H), 7.52 (d, 4H); FT-IR (KBr) ν (cm^{-1}): 3450，1620，1560，1410，1090，712.

Preparation of QAU-1. TPEP-2CBr (0.67 g) was dissolved in CH_3CN (20 mL), followed by the addition of triethylamine (2.02 g). The reaction mixture was slowly warmed up to 60 °C and stirred under Ar atmosphere overnight. The product was concentrated and purified through recrystallization in toluene solvent to afford QAU-1 as a white solid (yield, 81%). ^{1}H NMR (500 MHz, $CDCl_3$) δ (ppm): 1.28 (s, 18H), 3.38 (m, 12H), 4.5 (d, 4H), 7.25 (dd, 10H), 7.55 (m, 12H); FT-IR (KBr) ν (cm^{-1}): 3430，2980，1600，1560，1410，1090，812，768，710.

Preparation of AIE Dots-Based Probe. QAU-1 was dispersed in 10 mL phosphate buffer saline (PBS) (20 mM, pH 7.4), and the solution was then sonicated for 30 min to obtain a homogeneous dispersion. Subsequently, the AIE dots formed through the self assembling of QAU-1 in PBS. The obtained AIE dots were allowed to react with Q-DNA for 30 min to develop the AIE dots-based probe.

Fluorescence Detection of BLM. The BLM samples were pretreated by mixing BLM with Fe^{2+} in 1:1 molar ratio to form BLM-Fe^{2+} solution. In the typical assay, AIE dots-based probe, and a certain amount of BLM sample were mixed in 100 μL of reaction buffer and incubated at room temperature for 20 min before fluorescence measurements.

RESULTS AND DISCUSSION

Principle of AIE Dots-Based Probe. The working principle of the proposed biosensor is illustrated in Scheme 1. In our strategy, amphiphile QAU-1 was ingeniously designed, which comprised of tertaphenylethylene structure (hydrophobic part) and quaternary ammonium salt group (hydrophilic part). Under optimal circumstances, it could self-assemble into well-defined AIE dots, which emitted bright fluorescence, and possessed high positive charge densities on the surface, resulting in strong adsorption ability toward DNA through the electrostatic interaction (Scheme 1-I). Thus, AIE dots-based probe could be successfully prepared upon the addition of Q-DNA, and exhibited a negligible fluorescence emission

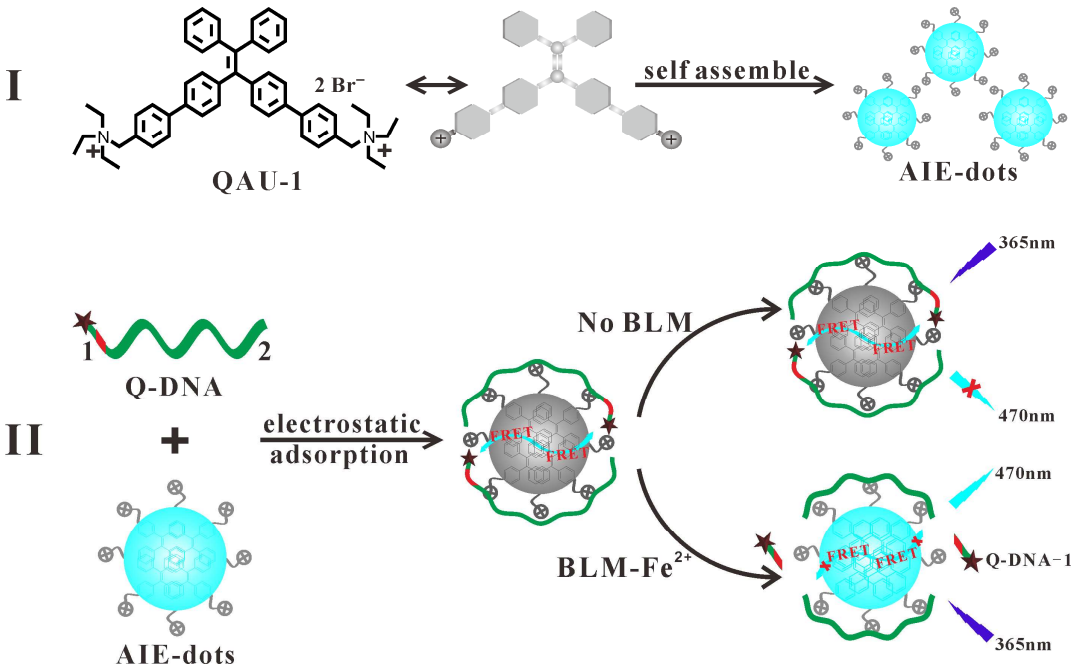

Scheme 1. (I) The schematic illustration of AIE dots preparation procedure, and (II) the principle of the proposed biosensor based on AIE dots to enhance fluorescence for ultrasensitive detection of BLM.

because of the FRET effect (Scheme 1-II). Certainly, Q-DNA, whose structure shown in Figure S1A, was rationally designed to consist of both a quencher and the target recognition sequence, i.e. GCT, toward BLM sample.[37,38] In the absence of BLM, Q-DNA could not be cleaved, and was still effectively anchored on AIE dots surface. Due to the FRET effect, which was dependent on the distance between the particular quencher in Q-DNA and AIE dots, weak fluorescence was observed for the AIE dots-based probe.[39,40] However, in the presence of BLM, Q-DNA was specifically cleaved at the scission site *via* the oxidative effect of BLM with Fe^{2+} as the cofactor, and three-mer quencher-linked oligonucleotide fragments (denoted as Q-DNA-1) were then released. As depicted in Figure S1B, the newly appeared band in lane b, at the longer distance than that of Q-DNA, was associated with the generation of 21-mer oligonucleotide fragments (denoted as Q-DNA-2), arising from the specific cleavage of Q-DNA by BLM-Fe^{2+}. Negative charge density in Q-DNA-1 drastically decreased and fewer Q-DNA-1 were anchored on AIE dots surface,

as compared to Q-DNA. Thus, the FRET effect from quencher to AIE dots was significantly weakened due to their relative long distance. Therefore, a remarkable fluorescence enhancement was readily observed. Because the FRET effect was dependent on the amount of Q-DNA anchored on the AIE dots surface, which was subsequently dependent on the concentration of BLM, the fluorescence enhancement of the as-proposed assay was thus related to the concentration of the target analyte, and ultrasensitive fluorescence detection of BLM was readily realized.

Characterization of AIE Dots-Based Probe. Amphiphile QAU-1 was prepared following the synthetic route depicted in Scheme S1 and the detailed steps for its synthesis were demonstrated in Experimental Section. The identities of QAU-1 and intermediates were firmly confirmed by ^{1}H NMR and FT-IR spectra (Figure S2). To evaluate the AIE behavior of QAU-1, we conducted fluorescence/UV-Vis measurements on QAU-1 in DMF-PBS mixture. As manifested in Figure 1A, when PBS fraction was ≤ 60%, QAU-1 exhibited weak fluorescence. However, with further increase of PBS content, prominent fluorescence response was observed, arising from the formation of QAU-1 aggregates and the subsequent restriction of intermolecular rotation. With the content of PBS reached 98%, a *ca.* 93.4-fold increase in intensity was observed. Meanwhile, owing to the low light transmission caused by Mie effect of the formed aggregates in mixed solution with PBS fraction ≥ 70% (Figure S3A), high absorbance in UV region and apparent levelling-off with low absorbance in the visible region were detected. Additionally, corresponding images of QAU-1 under UV irradiation with different PBS fractions were shown in Figure 1B, which further verified the fact that QAU-1 exhibits little fluorescence emission in molecule-dissolved state, and enjoys remarkable fluorescence emission in aggregate state. Moreover, the AIE characteristic of QAU-1 was also proven by performing its fluorescence in different solvents, *i.e.* good solvents and poor solvents, as shown in Figure S3B.

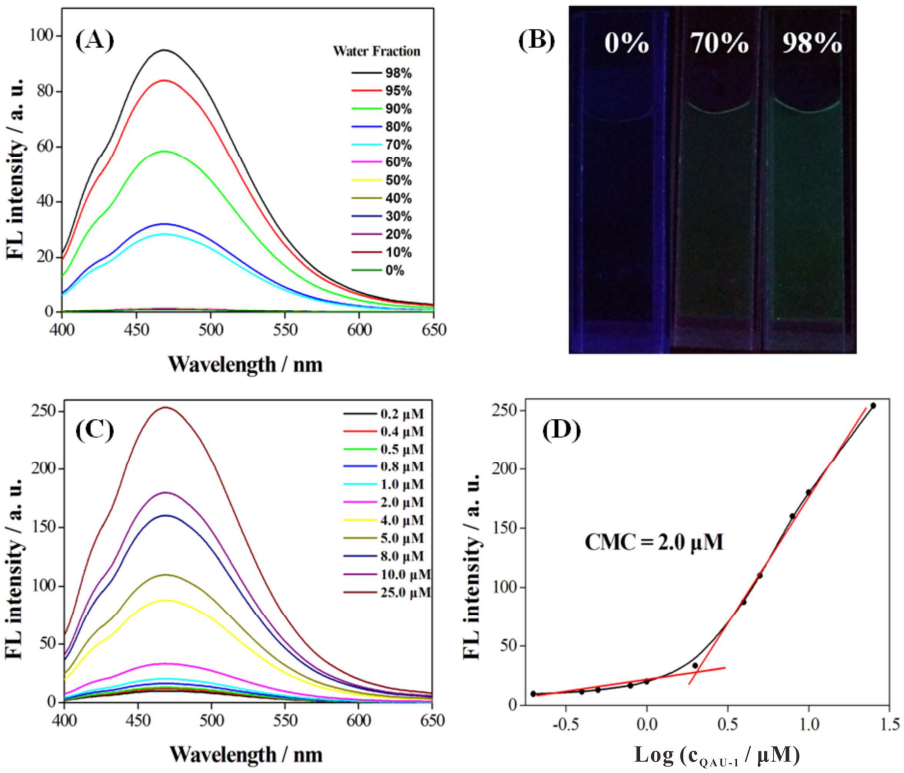

Figure 1. (A) Fluorescence emission spectra of QAU-1 (5 μM) in DMF-PBS mixtures. (B) Photographs of QAU-1 (5 μM) under 365 nm UV illumination in different PBS fractions. (C) Fluorescence spectra of QAU-1 with different concentrations in PBS. (D) Fluorescence intensity *vs.* the logarithm of QAU-1 concentration.

Organic nanoaggregates with well-defined morphologies and ultrasmall sizes have attracted unprecedented attention from scientists in recent years due to their application in numerous fields including chemo-/biosensors and photodynamic therapy.[41,42] However, to the best of our knowledge, AIE nanoaggregates with ultrasmall size (AIE dots) especially < 10 nm was scarcely reported. To address this challenge, herein a new strategy of self assembling of QAU-1 was adopted, and the self assembling process was thoroughly investigated by UV-Vis, FL and TEM techniques. Figure 1C shows the fluorescence spectra of PBS containing QAU-1 with different concentrations. When the concentration of QAU-1 was < 2 μM, the fluorescence intensity was very weak. Once the concentration of QAU-1 was ≥ 2 μM, the fluorescence intensity enhanced remarkably. This increase in intensity can be ascribed to the AIE effect triggered by the

formation of dots, in which the restriction of intermolecular rotation leads to elevated fluorescence. Meanwhile, the critical micelle concentration (CMC) value for QAU-1 was determined to be 2 μM through the changes of fluorescence intensity under different QAU-1 concentrations in PBS (Figure 1D). The formation of AIE dots can also be verified by UV-Vis spectra, which are demonstrated in Figure S3C.

The self assembling behaviour of QAU-1 was subsequently investigated by TEM, which helped in the visualization of the morphologies of the assembled AIE dots. Figure 2A-a gives a TEM micrograph of QAU-1 with the concentration of 0.2 μM. No nanoaggregates were obtained. Furthermore, spherical aggregates around 5 nm in diameter were clearly observed by TEM, with QAU-1 concentration further increased to 5 μM (Figure 2A-b, c), suggesting that QAU-1 self assembled into dots in PBS with the concentration ≥ 2 μM. Conversely, no nanoaggregates were detected in DMF with the concentration of 5 μM (Figure S3D). These implied that the AIE dots can only be prepared in PBS with the concentration larger than CMC, and are completely cleared from the organism during an acceptable period, and thus enjoy fascinating biocompatibility for advanced utilization in bioassay associated with human body.[33,34] For the potential application of AIE dots in chemo−/biosensing fields, the photostability and water dispersibility were further studied (Figure S3E and S3F). And the zeta potential value of AIE dots was determined to be 37.2 ± 3.1 mV, which was ascribed to the quaternary ammonium salt groups on the surface. These experimental results successfully implied that the prepared AIE dots enjoy excellent photostability and high resistance to photobleaching, and could maintain good stability for several weeks without precipitation formation.

In the present study, AIE dots were prepared through the self assembling of QAU-1 with the concentration of 5 μM in PBS, with the diameter of about 5 nm (Figure 2A-c) and high positive charge densities on the surface, which are beneficial for it to adsorb negatively charged DNA to develop bioassay. As shown in Figure 2B, the fluorescence intensity gradually declined with the increase of Q-DNA

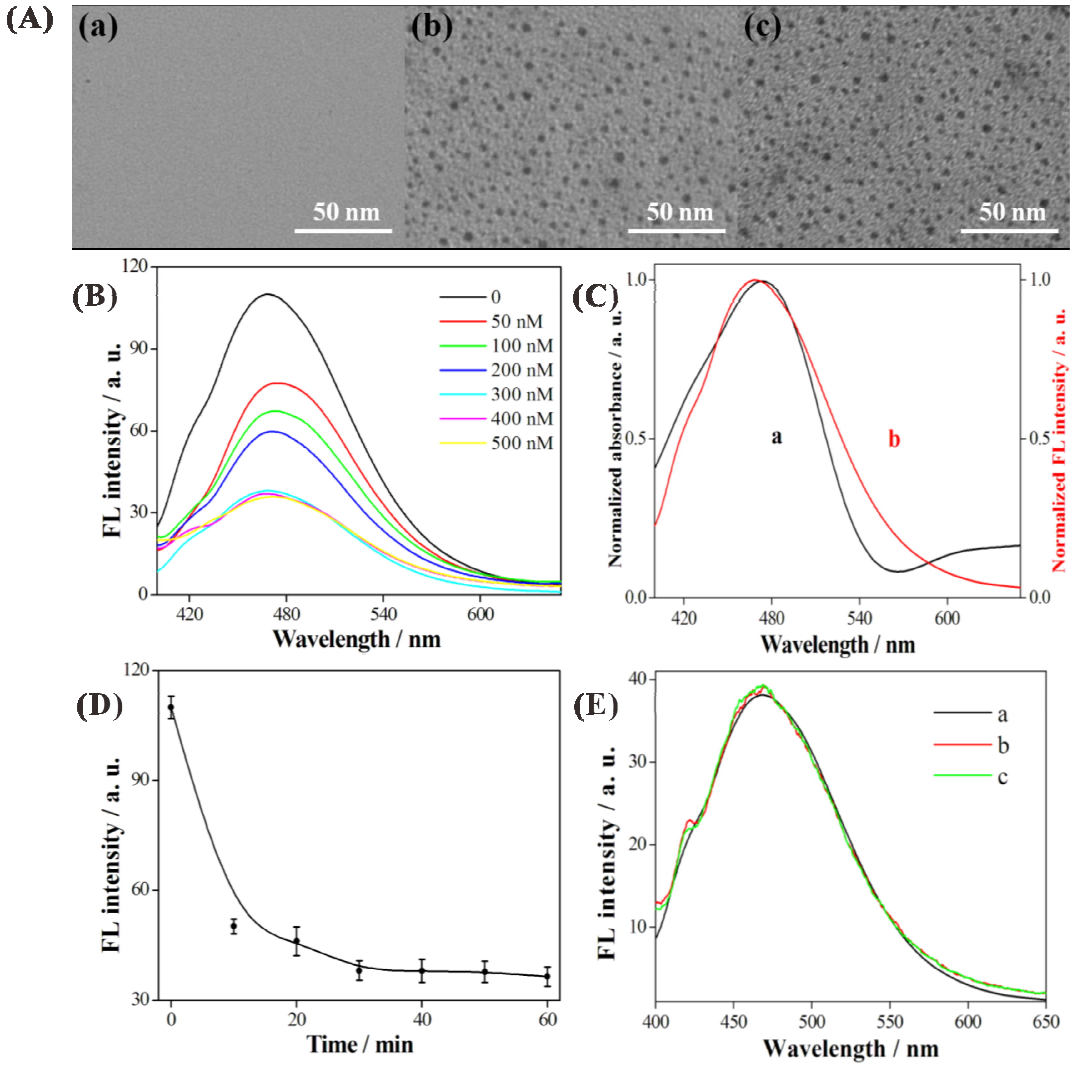

Figure 2. (A) TEM images of QAU-1 with different concentrations: (a) 0.2 μM, (b) 2.0 μM, (c) 5.0 μM. (B) Fluorescence spectra of AIE dots-based probe with different concentrations of Q-DNA (QAU-1, 5.0 μM). (C) The UV-Vis spectrum of Q-DNA (a) and fluorescence spectrum of AIE dots (b) in PBS. (D) Fluorescence intensity *vs.* the reaction time of AIE dots (5.0 μM) and Q-DNA (300 nM) in PBS. (E) Fluorescence spectra of AIE dots-based probe in (a) PBS, (b) PBS containing K^+, Mg^{2+}, Ca^{2+}, Cl^-, NO_3^-, (the concentrations of all ions were 100 nM), and (c) human serum sample (serum: PBS, 1: 3, v: v).

concentration from 0 to 300 nM, arising from the electrostatic adsorption and FRET effect between AIE dots and Q-DNA. The FRET effect was verified by the spectral overlap between the absorption spectrum of Q-DNA and the emission spectrum of AIE dots (Figure 2C). However, with the further increase of Q-DNA concentration, no obvious variations in intensity were detected, which could be attributed to the saturated

adsorption of Q-DNA. Thus, the optimal concentration of Q-DNA was chosen as 300 nM to develop this proposed assay, which is consistent with the zeta potential results shown in Figure S4A. Meanwhile, the incubation time for AIE dots-based probe preparation was also studied, and 30 min was selected as the optimal incubation time (Figure 2D). Prior to the application in detecting BLM, the stability of AIE dots-based probe was investigated. As illustrated in Figure 2E, no obvious change in fluorescence intensity was observed for AIE dots-based probe in PBS, PBS containing ions and serum sample, respectively, indicating that both ions and serum matrix have negligible interfering effect on the stability of the proposed probe.

To investigate such a DNA induced fluorescence turn-off phenomenon, the electrostatic interaction between AIE dots and Q-DNA was examined. The competitive adsorption experiment was designed by pre-incubation of Q-DNA with cationic polymer PDADMA, and subsequently adding AIE dots into the system (Figure 3A). The PDADMA masked the negative charges on Q-DNA, and thus blocked the binding of AIE dots to Q-DNA, resulting in no FRET effect. Thus, the fluorescence of AIE dots was not quenched. As depicted in Figure 3B, as compared to the case that PDADMA was absent, the pre-incubation of PDADMA with Q-DNA resulted in a fluorescence emission similar to that of AIE dots only, arising from the strong adsorption ability of the positively charged PDADMA toward Q-DNA and the subsequent absence of FRET effect between AIE dots and Q-DNA. To further confirm this, a structural analogue TPE-COOH, which has the same tertaphenylethylene core but is substituted with a carboxyl group, was used as a control (Figure 3C). It exhibited unique AIE characteristic, with significant fluorescence intensity observed in PBS, but hardly any fluorescence signal was detected in DMF (Figure S4B). Meanwhile, it exhibited the self-assembling behaviour (Figure S4C and S4D) for consisting of both hydrophobic part and hydrophilic part, and formed the aggregates in PBS with the concentration higher than the CMC value (15

μM). However, if TPE-COOH was used to substitute QAU-1 as the fluorogen, no obvious fluorescence decrease was detected after Q-DNA treatment (Figure 3D), which was due to the fact that the negatively charged TPE-COOH nanoaggregates cannot interact with Q-DNA because of the electrostatic repulsion effect, resulting in the separation of fluorogens and the quenchers and the subsequent reduction of FRET effect.

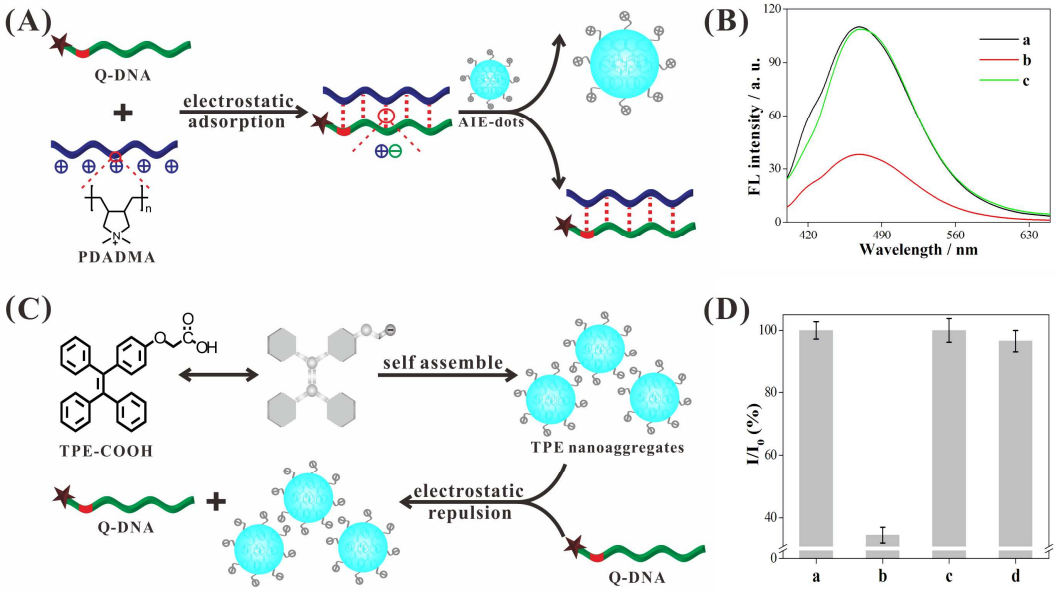

Figure 3. (A) Schematic illustration of the effect of PDADMA to prevent the formation of AIE dots-based probe. (B) Fluorescence spectra of AIE dots (5.0 μM) under different conditions: (a) AIE dots, (b) AIE dots + Q-DNA, (c) AIE dots + pre-incubated Q-DNA and PDADMA. (C) Schematic illustration of the TPE-COOH nanoaggregates formation and its electrostatic repulsion toward Q-DNA. (D) Comparison of the relative fluorescence changes of AIE dots (5.0 μM) and TPE nanoaggregates (25 μM) upon the addition of Q-DNA. For (a) and (b), I_0 and I are the fluorescence intensity of AIE dots before and after the addition of Q-DNA (300 nM). For (c) and (d), I_0 and I are the fluorescence intensity of TPE nanoaggregates before and after the addition of Q-DNA (1500 nM).

Feasibility Study of AIE Dots-Based Probe. To verify the feasibility of the proposed sensing strategy, fluorescence signals upon analyzing the target and those obtained in a series of control experiments were acquired and depicted in Figure 4A. Upon the addition of both BLM and Fe^{2+} with different concentrations, the fluorescence intensity elevated from 38.1 a. u. (a) to 52.3 a. u. (d) and 90.0 a. u.

(e), respectively. This is because a large amount of Q-DNA-1 formed upon the specific cleavage of Q-DNA by BLM-Fe^{2+}, which possessed significantly decreased adsorption ability and FRET effect toward AIE dots, thus resulting in the restoration of the fluorescence. Whereas, in the absence of BLM, Fe^{2+} or both, the fluorescence signals were about the same and fairly low (a, b and c). These experimental results clearly demonstrated that the fluorescence detection of target analyte could be readily achieved using the AIE dots-based probe.

In the proposed sensing strategy, fluorescence detection of a variety of analytes can be readily realized by simply changing the specific target recognition DNA sequences, thus, the design of Q-DNA is very important for BLM probing and was investigated. Two DNA strands, namely P1 and P2, with their sequences shown in Table S1, were designed and substituted Q-DNA in the proposed assay. As compared to Q-DNA, P1 did not contain the specific sequences recognizable by BLM, and P2 was not labelled with the quencher molecule. As manifested in Figure S5, with Q-DNA substituted by P1, the proposed biosensor exhibited similar fluorescence intensity as that using Q-DNA, but in the presence of BLM, little fluorescence intensity change was observed. Whereas, with Q-DNA substituted by P2, the probe emitted much brighter fluorescence because of the absence of the quencher, and similar to the case of P1, no obvious fluorescence intensity variation was observed when BLM was present.

Analytical Performance of AIE Dots-Based Probe. Under the optimum experimental conditions (Figure S6), we challenged this fluorescence biosensor by probing target BLM with different concentrations to test its sensing performance. As illustrated in Figure 4B, the fluorescence intensity remarkably augmented with the increase of BLM concentration, which could be ascribed to the fact that more BLM impelled the generation of more Q-DNA-1, with declined adsorption ability and FRET effect toward AIE dots. A calibration curve made by plotting ΔI *vs.* the BLM concentration (c_{BLM}) is exhibited in

Figure 4C. It is clearly shown that ΔI was linearly proportional to the logarithm of c_{BLM} within two ranges, *i.e.* 0.01 to 500 pM (Figure 4D) and 1000 to 500000 pM (Figure 4E), respectively. In the low concentration linear range, the resulting regression equation was determined as $\Delta I = 3.017 \log c_{BLM} + 6.672$ (ΔI in the units of a. u., c_{BLM} in the units of pM), and in the high concentration linear range, the regression equation was $\Delta I = 12.09 \log c_{BLM} - 17.60$ (ΔI in the units of a. u., c_{BLM} in the units of pM), with the correlation coefficient of $R^2 = 0.9893$ and $R^2 = 0.9924$, respectively. Accordingly, the detection limit was calculated to be 3.4 fM (based on signal-to-noise ratio of 3), which, as shown in Table S2, to the best of our knowledge, was the lowest detection limit ever obtained for BLM detection.

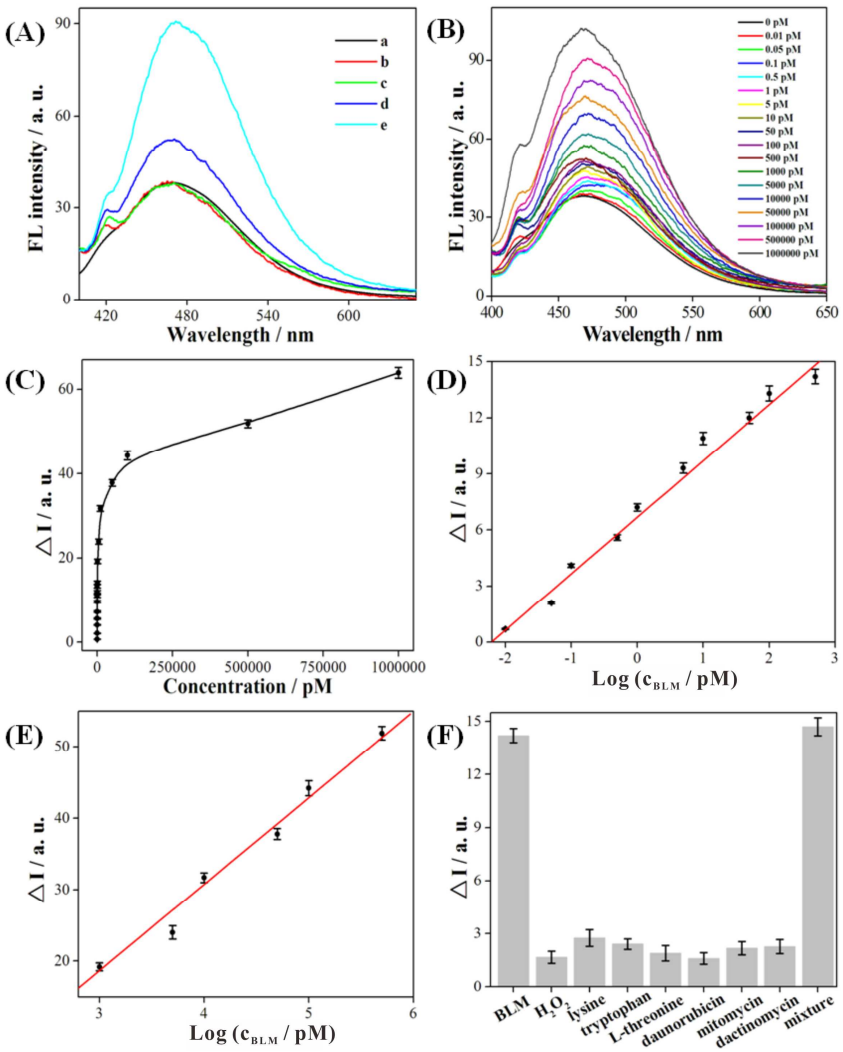

Figure 4. (A) Fluorescence spectra of proposed biosensor under different conditions: (a) AIE dots-based probe, (b) AIE dots-based probe + BLM (500 pM), (c) AIE dots-based probe + Fe^{2+} (500 pM), (d) AIE dots-based probe + BLM-Fe^{2+} (500 pM), (e) AIE dots-based probe + BLM-Fe^{2+} (500 nM). (B) Fluorescence spectra of proposed biosensor upon the addition of BLM with different concentrations. (C) The fluorescence intensity change (ΔI) of the proposed biosensor before and after the addition of BLM *vs.* the BLM concentration. (D) The linear plot of ΔI *vs.* the logarithm of the BLM concentration ranging from 0.01 to 500 pM. (E) The linear plot of ΔI *vs.* the logarithm of the BLM concentration ranging from 1000 to 500000 pM. (F) Comparison of ΔI in the presence of BLM, H_2O_2, lysine, tryptophan, *L*-threonine, daunorubincin, mitomycin, dactinomycin, and the mixture of these substances, respectively. $\Delta I = I - I_0$, where I is the fluorescence intensity in the presence of BLM or one of the seven interfering substances, and I_0 is the fluorescence intensity of AIE dots-based probe. The concentrations of all analytes were 500 pM.

Selectivity of AIE Dots-Based Probe. To investigate the selectivity of the proposed fluorescence biosensor for BLM assay, seven other compounds, namely, daunorubincin, mitomycin, dactinomycin, H_2O_2,

lysine, tryptophan, and *L*-threonine, were added into the sensing system as the interfering substances. As shown in Figure 4F, obvious fluorescence response was detected only in the presence of BLM, whereas, little variation in intensity was observed in the presence of one of the seven interfering substances. Furthermore, a 500 pM BLM sample containing the seven interfering substances exhibited no obvious change, as compared with that acquired in the sample containing 500 pM BLM only. Thus, the proposed fluorescence biosensor demonstrated excellent performance for distinguishing BLM against other interfering substances.

Real Sample Analysis. Finally, we tested the AIE dots-based assay for BLM detection in clinical samples through the recovery experiments by spiking BLM-Fe^{2+} with different concentrations into human serum samples. As manifested in Table S3, for BLM with different concentrations of 1, 20 and 200 pM, there was good agreement between the added and the measured values of BLM concentrations, with the recoveries in the range of 99.12% to 103%, implying no severe interferences in clinical samples. Moreover, the relative standard deviations (RSD) of three repetitive measurements for these samples were all below 3.3%, demonstrating good reproducibility. These results arguably indicated that the proposed fluorescence bioassay had good reliability and reproducibility, and could be successfully utilized for the detection of BLM in clinical samples.

CONCLUSIONS

In this work, we reported a general strategy to prepare highly fluorescent AIE dots with exceptional colloidal stability, ultrasmall size, and functional groups that allow for electrostatic conjugation to biological molecules, and we also demonstrated their application in developing ultrasensitive fluorescence bioassay. Due to the efficient FRET effect between AIE dots and the quenchers labelled on biological molecules, the fluorescence of the proposed biosensor was initially quenched, and a turn-on signal was

sequentially observed upon the addition of BLM, the proof-of-concept target analyte. The proposed biosensor exhibited ultrahigh sensitivity, and a detection limit down to 3.4 fM was obtained, which is the lowest value reported so far. The applicability of this fluorescence biosensor for real sample analysis has also been demonstrated by probing BLM spiked in human serum samples. Moreover, ultrasensitive detection of other analytes can be readily achieved by simply changing the specific target recognition substrate, thus providing a versatile fluorescence platform for ultrasensitive detection of a variety of biomolecules. Therefore, the proposed fluorescence bioassay has great potential to be applied in the areas of bioanalysis and clinical biomedicine.

Notes

The authors declare no competing financial interest.

ACKNOWLEDGEMENTS

This work was funded by the National Natural Science Foundation of China (Nos. 21575074, 21605093 and 21675095), the Project of Shandong Province Higher Educational Science and Technology Program (No. J15LC08), and the Special Foundation for Distinguished Taishan Scholar of Shandong Province (No. ts201511052).

Supporting Information

Reagents and apparatus; synthetic route of QAU-1; ^{1}H NMR and FT-IR spectra; absorption, fluorescence, zeta potential, and TEM data; BLM assay performance comparison of our strategy with other methods; detection of BLM spiked in serum samples.

REFERENCES

(1) Cosnier, S.; Holzinger, M. *Chem. Soc. Rev.* **2011**, *40*, 2146–2156.

(2) Rackus, D. G.; Shamsi, M. H.; Wheeler, A. R. *Chem. Soc. Rev.* **2015**, *44*, 5320–5340.

(3) Kim, S. N.; Rusling, J. F.; Papadimitrakopoulos, F. *Adv. Mater.* **2007**, *19*, 3214–3228.

(4) Saqib, M.; Gao, W.; Lai, J. P.; Qi, L. M.; Majeed, S.; Gilani, M. R. H. S.; Xu, G. B. *Chem. Commun.* **2015**, *51*, 6536–6539.

(5) Freeman, R.; Liu, X. Q.; Willner, I. *J. Am. Chem. Soc*. **2011**, *133*, 11597–11604.

(6) Nepomnyashchii, A. B.; Bard, A. J. *Acc. Chem. Res*. **2012**, *45*, 1844–1853.

(7) Zhao, M.; Chen, A.-Y.; Huang, D.; Zhuo, Y.; Chai, Y. Q.; Yuan, R. *Anal. Chem*. **2016**, *88*, 11527–11532.

(8) Li, H. Y.; Chang, J. F.; Hou, T.; Li, F. *Anal. Chem*. **2017**, *89*, 673–680.

(9) Kirsch, J.; Siltanen, C.; Zhou, Q.; Revzin, A.; Simonian, A. *Chem. Soc. Rev*. **2013**, *42*, 8733–8768.

(10) Shi, H. F.; Sun, H. B.; Yang, H. R.; Liu, S. J.; Jenkins, G.; Feng, W.; Li, F. Y.; Zhao, Q.; Liu, B.; Huang, W. *Adv. Funct. Mater.* **2013**, *23*, 3268–3276.

(11) Tang, B.; Xing, Y. L.; Li, P.; Zhang, N.; Yu, F. B.; Yang, G. W. *J. Am. Chem. Soc*. **2007**, *129*, 11666–11667.

(12) Xiao, H. B.; Li, P.; Hu, X. F.; Shi, X. H.; Zhang, W.; Tang, B. *Chem. Sci*. **2016**, *7*, 6153–6159.

(13) Lacour, W.; Adjili, S.; Blaising, J.; Favier, A.; Monier, K.; Mezhoud, S.; Ladavière, C.; Place, C.; Pécheur, E.-I.; Charreyre, M.-T. *Adv. Healthc. Mater.* **2016**, *5*, 2032–2044.

(14) Li, H. Y.; Wang, C. F.; Gai, P. P.; Hou, T.; Ge, L.; Li, F. *RSC Adv*. **2016**, *6*, 76679–76683.

(15) Freage, L.; Wang, F.; Orbach, R.; Willner, I. *Anal. Chem*. **2014**, *86*, 11326–11333.

(16) Mei, J.; Leung, N. L. C.; Kwok, R. T. K.; Lam, J. W. Y.; Tang, B. Z. *Chem. Rev.* **2015**, *115*, 11718–11940.

(17) Mei, J.; Hong, Y. H.; Lam, J. W. Y.; Qin, A. J.; Tang, Y. H.; Tang, B. Z. *Adv. Mater.* **2014**, *26*, 5429–5479.

(18) Zhang, X. Y.; Wang, K.; Liu, M. Y.; Zhang, X. Q.; Tao, L.; Chen, Y. W.; Wei, Y. *Nanoscale.* **2015**, *7*, 11486–11508.

(19) Kim, S.; Ohulchanskyy, T. Y.; Pudavar, H. E.; Pandey, R. K.; Prasad, P. N. *J. Am. Chem. Soc*. **2007**, *129*, 2669–2675.

(20) Rao, P. H.; Yao, W.; Li, Z. C.; Kong, L.; Zhang, W. Q.; Li, L. *Chem. Commun.* **2015**, *51*, 8757–8760.

(21) Li, H. Y.; Zhang, X. Q.; Zhang, X. Y.; Wang, K.; Liu, H. L.; Wei, Y. *ACS Appl. Mater. Interfaces.* **2015**, *7*, 4241–4246.

(22) Yu, J. B.; Rong, Y.; Kuo, C. T.; Zhou, X. H.; Chiu, D. T. *Anal. Chem*. **2017**, *89*, 42–56.

(23) Wu, C. F.; Chiu, D. T. *Angew. Chem. Int. Ed.* **2013**, *52*, 3086–3109.

(24) Ma, C. P.; Ling, Q. Q.; Xu, S. D.; Zhu, H. N.; Zhang, G.; Zhou, X.; Chi, Z. G.; Liu, S. W.; Zhang, Y.; Xu, J. R. *Macromol. Biosci.* **2014**, *14*, 235–243.

(25) Ding, D.; Mao, D.; Li, K.; Wang, X. M.; Qin, W.; Liu, R. R.; Chiam, D. S.; Tomczak, N.; Yang, Z. M.; Tang, B. Z.; Kong, D.; Liu, B. *ACS Nano.* **2014**, *8*, 12620–12631.

(26) Wang, G. T.; Tang, B. H.; Liu, Y.; Gao, Q. Y.; Wang, Z. Q.; Zhang, X. *Chem. Sci*. **2016**, *7*, 1151–1155.

(27) Shi, B. B.; Jie, K. C.; Zhou, Y. J.; Zhou, J.; Xia, D. Y.; Huang, F. H. *J. Am. Chem. Soc*. **2016**, *138*, 80–83.

(28) Luo, J. D.; Xie, Z. L.; Lam, J. W. Y.; Cheng, L.; Chen, H. Y.; Qiu, C. F.; Kwok, H. S.; Zhan, X. W.; Liu, Y. Q.; Zhu, D. B.; Tang, B. Z. *Chem. Commun.* **2001**, 1740–1741.

(29) Li, H. Y.; Chi, Z. G.; Zhang, X. Q.; Xu, B. J; Liu, S. W.; Zhang, Y.; Xu, J. R. *Chem. Commun.* **2011**, *47*, 11273–11275.

(30) Liu, L. J.; Li, H.; Bian, J.; Qian, J. Y.; Wei, Y. J.; Li, J.Y.; Tian, W. J. *New J. Chem*. **2014**, *38*, 5009–5017.

(31) Wang, Z. K.; Chen, S. J.; Lam, J. W. Y.; Qin, W.; Kwok, R. T. K.; Xie, N.; Hu, Q. L.; Tang, B. Z. *J. Am. Chem. Soc*. **2013**, *135*, 8238–8245.

(32) Xu, S. Y.; Bai, X. L.; Ma, J. W.; Xu, M. M.; Hu, G. F.; James, T. D.; Wang, L. Y. *Anal. Chem*. **2016**, *88*, 7853–7857.

(33) Sun, Z. B.; Xie, H. H.; Tang, S. Y.; Yu, X.-F.; Guo, Z. N.; Shao, J. D.; Zhang, H.; Huang, H.; Wang, H. Y.; Chu, P. K. *Angew. Chem. Int. Ed.* **2015**, *54*, 11526–11530.

(34) Yildirimer, L.; Thanh, N. T. K.; Loizidou, M.; Seifalian, A. M. *Nano. Today.* **2011**, *6*, 585–607.

(35) Wu, C. F.; Schneider, T.; Zeigler, M.; Yu, J. B.; Schiro, P. G.; Burnham, D. R.; McNeill, J. D.; Chiu, D. T. *J. Am. Chem. Soc*. **2010**, *132*, 15410–15417.

(36) Mandal, K.; Jana, D.; Ghorai, B. K.; Jana, N. R. The *J. Phys. Chem. C*. **2016**, *120*, 5196–5206.

(37) Gao, F. L.; Lei, J. P.; Ju, H. X. *Chem. Commun*. **2013**, *49*, 7561–7563.

(38) Li, F.; Feng, Y.; Zhao, C.; Li, P.; Tang, B. *Chem. Commun.* **2012**, *48*, 127–129.

(39) Ou, M.; Huang, J.; Yang, X. H.; Quan, K.; Yang, Y. J.; Xie, N. L.; Wang, K.M. *Chem. Sci*. **2017**, *8*, 668–673.

(40) Yuan, Y. Y.; Zhang, R. Y.; Cheng, X. M.; Xu, S. D.; Liu, B. *Chem. Sci*. **2016**, *7*, 4245–4250.

(41) Xiong, L. Q.; Shuhendler, A. J.; Rao, J. H. *Nat. Commun.* **2012**, *3*, 1193–1201.

(42) Pu, K. Y.; Mei, J. G.; Jokerst, J. V.; Hong, G. S.; Antaris, A. L.; Chattopadhyay, N.; Shuhendler, A. J.; Kurosawa, T.; Zhou, Y.; Gambhir, S. S.; Bao, Z. N.; Rao, J. H. *Adv. Mater.* **2015**, *27*, 5184–5190.

For TOC only

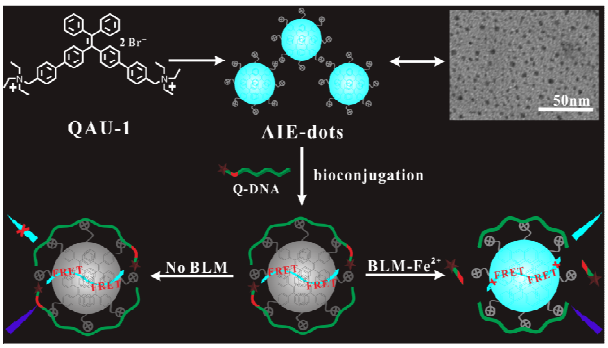
2 Br⁻
QAU-1
AIE-dots
50nm
Q-DNA
bioconjugation
No BLM
BLM-Fe³⁺
FRET
FRET
FRET
FRET
FRET
FRET